Supplementary Information, Scanning DMA Data Analysis I. Classification Transfer Function

Huajun Mai*and Richard C. Flagan*†‡

1 COMSOL simulation

1.1 Fluid flow field and electric field simulations

The configuration of the TSI Model 3081A long-column DMA, shown in the Figure 1 of the main text, was subdivided into entrance, classification and exit regions to perform particle trajectories simulations individually. Both the entrance and exit regions are grounded; the fluid flow field in these regions, which have non-axisymmetric elements, were simulated as a 3-dimensional, steady-state, laminar flow using COMSOL Multiphysics^{TM} . Fig. S1 shows the sectional view of the fluid flow profile for an aerosol flow of $Q_a = 0.51$ LPM (liters per

*Division of Engineering and Applied Science, California Institute of Technology, Pasadena, California 91125, USA

†Division of Chemistry and Chemical Engineering, California Institute of Technology, Pasadena, California 91125,USA

‡Corresponding author: flagan@caltech.edu

minute) through the DMA entrance region. The flow at the entrance to the curved aerosol inlet tube on the DMA was assumed to be fully-developed and laminar, while an atmospheric pressure boundary condition was prescribed at the annular outflow boundary. The no-slip condition is applied to all the other boundaries.

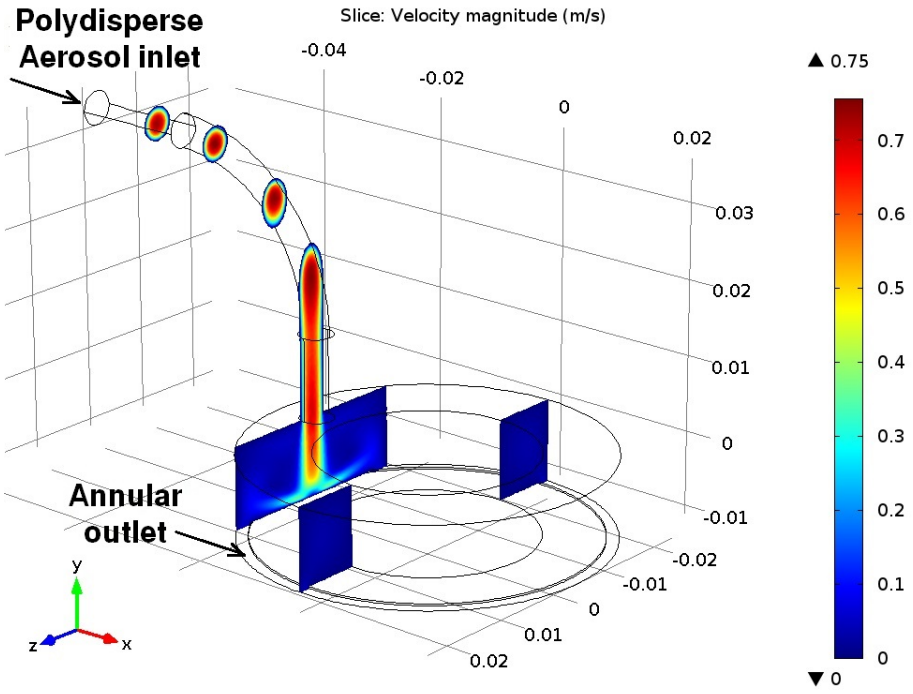

Figure S1: Section view of fluid flow velocity magnitude within the DMA entrance region at $z = -0.045, -0.035, -0.025, -0.019, 0$ m.

Fig. S2 shows flow field within the the DMA exit, downstream of the adverse potential gradient region. The flow field simulation extends part of the way into the central tube flow region where at the end of the extended classification region so that the fully developed fluid flow is reproduced at the entrance to the exit region. Recirculation can be observed at the bottom of the cone where the incoming flow impinges on the wall before entering the classified aerosol outlet section.

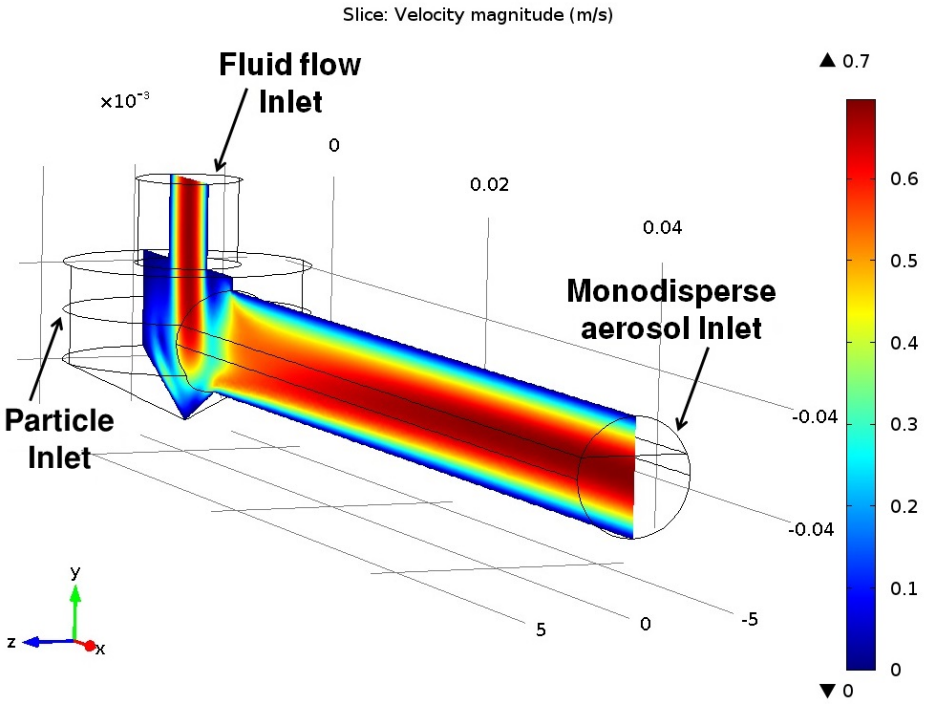

Figure S2: Section view of fluid flow velocity magnitude within the DMA exit region at $z = 0$ m. Notice that the fluid flow simulation is extended into the classification region to calculate the accurate fluid flow field within the exit region.

To facilitate the Brownian dynamics simulations of the particle trajectories within the DMA, the classification region was subdivided into 11 zones as shown in Fig. S3 and simulated as a two-dimensional, axisymmetric flow. The velocity and electric fields from the triangular mesh in each of these zones of the COMSOL^{TM} simulations were interpolated onto a quadrilateral grid for use in the Brownian dynamics simulations. As shown in the top inset, grid spacings were nonuniform to capture the boundary layer regions of the flow, and non-rectilinear where necessary to follow the shapes of the boundaries, as illustrated in the lower inset.

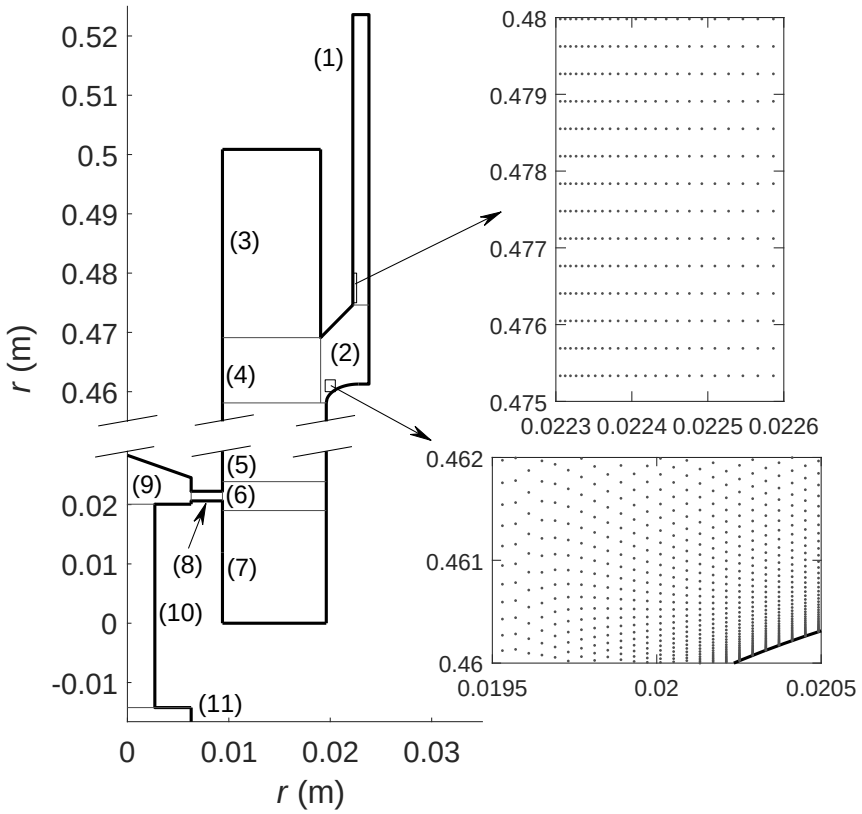

Figure S3: Segmentation of the exact classification region, with zone indices labled. Inset shows the interpolation grids for the fluid flow field and the electric field.

1.2 Particle trajectory simulation

The particle trajectory simulations in the DMA entrance and exit regions were completed by applying the COMSOL Multiphysics^{TM} 5.0 particle tracing module to the fluid flow fields and quasi-steady-state electric fields that had previously been obtained. The COMSOL Multiphysics^{TM} 5.0 particle tracing module does not account for non-continuum effects, *i.e.*, there is provision for including a slip correction factor. Therefore, an equivalent particle size method was used to account for the non-continuum effects of drag force and Brownian

diffusion simultaneously, *i.e.*, the pseudo particle diameter as simulation input is $D_{\mathrm{p,sim}} = D_{\mathrm{p}}/C_{\mathrm{c}}(D_{\mathrm{p}})$, where D_{p} is actual particle diameter, and $C_{\mathrm{c}}(D_{\mathrm{p}})$ is the Cunningham correction factor.

The efficiency of penetration through the entrance region was evaluated as

$$\eta_{\mathrm{ent}}(D_{\mathrm{p}}) = \frac{N_{\mathrm{out}}}{N_{\mathrm{in}}}, \tag{1}$$

where D_{p} is the electric mobility equivalent particle diameter, N_{out} is number of particles reaching the outflow boundary, and N_{in} is the number of particles injected to the inflow boundary. For simulations at each particle size, 10^5 particles were supplied to the inflow boundary, with a particle density proportional to the fluid volumetric flux.

The time-dependent penetration efficiency for each size and time was evaluated at the time when particles leave the exit region, *i.e.*,

$$\eta_{\mathrm{exit}}(D_{\mathrm{p}}, t) = \frac{N_{\mathrm{out}}(t)}{N_{\mathrm{in}}}, \tag{2}$$

where $N_{\mathrm{out}}(t)$ is number of particles reaching the outlet boundary at time t since the particles enter the DMA exit region. Due to the wall deposition, the overall penetration for a given particle size can not exceed unity, *i.e.*, $\int_0^\infty \eta_{\mathrm{exit}}(D_{\mathrm{p}}, t)\mathrm{d}t \leq 1$ for any D_{p}.

2 Brownian dynamics in cylindrical coordinates

Equation (8) in Part I shows the radial component of particle motion in cylindrical coordinates, based on the sketch shown in Fig. S4. The radial motion combines the Brownian contributions in the x and y directions, $\mathrm{d}\sigma_x^2 = \mathrm{d}\sigma_y^2 = 2\mathcal{D}\mathrm{d}t$, into the r component. The

radial position of the particle as a function of time is, therefore,

$$r(t+\mathrm{d}t) = \sqrt{\left[r(t) + \int_{t}^{t+\mathrm{d}t} v_r(r,z,t)\mathrm{d}t + g\left(\sqrt{\mathrm{d}\sigma_x^2}\right)\right]^2 + g\left(\sqrt{\mathrm{d}\sigma_y^2}\right)^2}. \tag{3}$$

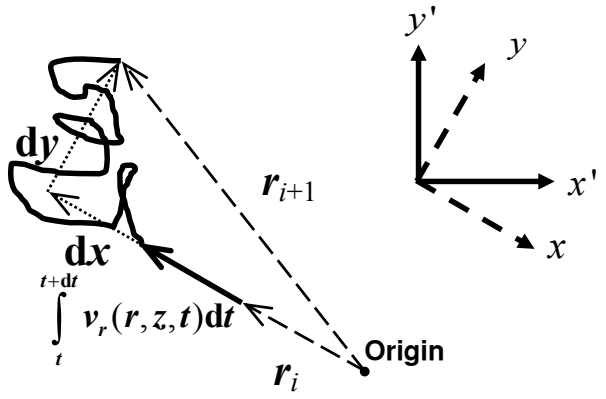

Figure S4: Particle motion in radial direction. $\int_{t}^{t+\mathrm{d}t} v_r(r,z,t)\mathrm{d}t$ denotes the migration in the fluid flow field and electric field, and $\mathrm{d}x$ and $\mathrm{d}y$ denote the displacement due to Brownian motion.